

# Quantitative structure–activity relationship analysis of a series of 2,3-diaryl benzopyran analogues as novel selective cyclooxygenase-2 inhibitors

S. Prasanna, E. Manivannan and S. C. Chaturvedi\*

*School of Pharmacy, Devi Ahilya Vishwavidyalaya, Indore 452017, Madhya Pradesh, India*

Received 20 March 2004; revised 18 May 2004; accepted 19 May 2004

Available online 19 June 2004

**Abstract**—A series of recently synthesized 2,3-diaryl benzopyrans reported as novel selective cyclooxygenase-2 inhibitors was subjected to quantitative structure–activity relationship (QSAR) analysis. Our attempt in correlating the derived physicochemical properties with the COX-2 inhibitory activity resulted in some statistically significant QSAR models with good predictive ability. The QSAR results and the probable pharmacophore features investigated through our study explored some interesting findings for the design of potent new class of selective COX-2 inhibitors.

© 2004 Elsevier Ltd. All rights reserved.

Conventional nonsteroidal anti-inflammatory drugs (NSAIDs) are profoundly used in the treatment of wide variety of inflammatory conditions including osteoarthritis and rheumatoid arthritis. However, the chronic use of these agents has been pointed out in induction of several gastro intestinal (GI) adverse effects.<sup>1</sup> NSAIDs act by inhibition of cyclooxygenase (COX), the enzyme involved in the biosynthesis of prostaglandins, prostacyclins and thromboxanes from arachidonic acid. COX exists in two isoforms, COX-1 primarily responsible for cytoprotection and COX-2, the inducible form associated with inflammation.<sup>2–4</sup> The hypothesis that the GI toxicity is due to COX-1 inhibition and desired anti-inflammatory activity is mediated by COX-2 inhibition led to the search of selective COX-2 inhibitors<sup>5–7</sup> such as celecoxib, rofecoxib, and valdecoxib.

Since last decade ample of QSAR studies of different heterocyclic ring systems (Fig. 1) as selective COX-2 inhibitors have been studied.<sup>8–12</sup> Recently Hansch et al., reported a comprehensive comparative QSAR study of COX inhibitors.<sup>13</sup> It provides plentiful information apropos to steric, electronic, and hydrophobic requirements of terphenyls, cyclopentenes, oxazoles, pyrazoles,

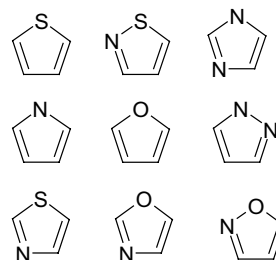


**Figure 1.** Different heterocyclic rings studied as selective COX-2 inhibitors.

pyrroles, imidazoles, thiophenes, oxazolones, pyridines, and other fused ring systems for selective COX-2 inhibition. Recently a novel series<sup>14</sup> of selective COX-2 inhibitors having a central scaffold with naturally occurring flavone was reported by Y. H. Joo et al. No QSAR work has been done till date on this class of compounds as it is being the first time to introduce 2,3-diaryl benzopyran lead structure as a part of the diaryl heterocyclic family of selective COX-2 inhibitors. Most of the structural variations of the congeneric series are attributed to the 3-aryl ring. The changes include F, Cl, methyl phenyl substituents to naphthyl, benzo[b]thiophenyl, and methylene dioxy phenyl rings. A minor modification of =O and =S at 4-position of the lead structure is also identified. The research group, Y. H. Joo et al. concluded that the introduction of a halogen

**Keywords:** COX-2; COX-1; QSAR; MOE.

\* Corresponding author. Tel.: +91-0731-2460976; e-mail: [prasu05@rediffmail.com](mailto:prasu05@rediffmail.com)

atom on the 3-aryl ring resulted in best COX-2 inhibitory activity whereas a big steric bulk on the same position resulted in least inhibitory activity. It is realized noteworthy in quantifying aforementioned structure–activity data and exploring the nature of interactions of these novel ligands with the COX-2 enzyme. In the light of the above set sights, we subjected the title compounds for QSAR analysis.

All the computational works were performed on molecular operating environment (MOE 2002.03), supplied by the Chemical Computing Group Inc., using Compaq Pentium 4 workstation. The correlation analysis of various physicochemical descriptors and biological activity data was accomplished by systat version 10.2.

Structures of all compounds were sketched using molecular builder of MOE and each structure was subjected to energy minimization upto a gradient of 0.01 kcal/mol Å using the MMFF94 force field. Three optimization methods were used in succession namely first steepest descent, then conjugate gradient and finally truncated Newton.

Conformational search of each energy-minimized structure was performed using stochastic approach. Stochastic conformational search method is similar to the RIPS method, which generate new molecular conformation by randomly perturbing the position of each coordinate of each atom in the molecule followed by the energy minimization. All conformers generated for each structure were analyzed in conformational geometries panel with great care and the lowest energy conformation of each structure was selected and saved into a database for descriptor calculation.

QuaSAR-descriptor module of MOE was used to calculate about 180 descriptors for each molecule. The calculated descriptors are partitioned into three classes: 2D descriptors, which use the atoms and connection information of the molecules, internal 3D (i3D), which use 3D coordinate information about each molecule and external 3D (x3D), which use 3D coordinate information with an absolute frame of reference.

The most active molecule of the training set compounds has been selected as the template for superimposition of all other members of the congeneric series. MOE-Flex align is a stochastic search procedure that simultaneously searches the conformation space of a collection of molecules and the space of alignment of those molecules. The probability density functions used are gaussians. The RMSD tolerance was set to 0.5.

Regression analysis was performed using COX-2 inhibitory activity as dependent variable and the calculated descriptors as predictor variables. Pruning of the large number of calculated descriptors<sup>15</sup> was aided by QuaSAR—contingency analysis of MOE. QSAR models were derived after ensuring reasonable correlation of COX-2 inhibitory activity with the individual descriptors and minimum intercorrelation among the descrip-

tors used in the derived models. Multicollinearity problem between the descriptors used in the derived models was tested using variance inflation data (VIF). Larger values of VIF (>10, corresponding to  $r^2 > 0.9$ ) indicate problems with collinearity. The quality of the models was assessed using the statistical parameters viz., correlation coefficient ( $r$ ) or coefficient of determination ( $r^2$ ), standard error of estimate ( $s$ ), Fischer  $F$ -value, and student's  $t$ -distribution. The latter is used to assess the significance of the individual regression terms. The figures within the parentheses following the coefficient terms are the standard error of the regression terms and the constants. The predictor variables with  $p$  value greater than 0.05 were eliminated whilst deriving the QSAR models in order to assure its statistical reliability. The Durbin–Watson (DW) statistic tests the residuals to determine if there is any significant correlation based on the order in which they occur. The DW value of greater than 1.4 is taken as the indication for the absence of any serious autocorrelation in the residuals. Model Z score (absolute difference between the values of the model and the activity field, divided by the square root of the mean square error of the data set) was taken as a measure of outlier detection. In order to corroborate the self-consistency of the derived models, they were validated using leave-one-out (LOO) process and the predictability of each model was assessed using cross-validated  $r^2$  or  $q^2$ .

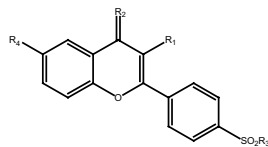
All the 26 compounds used for the study under training set are enumerated in Table 1. The structures of four compounds with converted percentage inhibition of COX-2 enzyme for test set is indicated in Table 2. The descriptors used in the models are listed in Table 3. The reported in vitro COX-2 enzyme inhibitory activity data ( $IC_{50}$  in  $\mu\text{g/mL}$ ) of training set was converted to negative logarithm in  $\mu\text{molar}$  units ( $pIC_{50}$ ), where  $IC_{50}$  represents the drug concentration that inhibits 50% of the COX-2 enzyme. The reported percentage inhibition values in  $\mu\text{g/mL}$  of test set molecules are converted to  $\log P/100 - P$ , where  $P$  represents the percentage inhibition. The COX-2 inhibitory activity retained for the study was obtained from the mouse peritoneal macrophage method. In order to explore the nature of interactions of  $R_1$ ,  $R_2$ ,  $R_3$ , and  $R_4$  groups with the amino acid residues of COX-2 active site, statistically significant QSAR models were developed. The best simple linear correlation obtained through multiple regression equations are discussed below.

#### Model-1

$$pIC_{50} = 0.336(\pm 0.138)a_{nS} - 0.047(\pm 0.010)S \log P_{\text{VSA1}} - 0.013(\pm 0.003)rdw_{\text{vol}} + 12.258(\pm 1.624)$$

$$n = 26, r = 0.826, r^2 = 0.683, s = 0.269, \\ F_{3,22} = 15.79, q^2 = 0.5765, \text{Spress} = 0.311, \\ \text{SDEP} = 0.286, p = 0.000$$

The tri parametric model-1 explains 68.3% variance in activity. The standard error of estimate of the derived

**Table 1.** Structures of 2,3-diaryl benzopyrans and their COX-2 inhibitory activity (training set)

No.	Substitution				$pIC_{50}$
	$R_1$	$R_2$	$R_3$	$R_4$	
1		O	CH <sub>3</sub>	H	3.03
2		O	CH <sub>3</sub>	H	3.69
3		O	CH <sub>3</sub>	H	4.12
4		O	CH <sub>3</sub>	H	3.27
5		O	CH <sub>3</sub>	H	3.47
6		O	CH <sub>3</sub>	H	3.44
7		O	CH <sub>3</sub>	H	3.44
8		O	CH <sub>3</sub>	H	3.57
9		O	CH <sub>3</sub>	H	3.29
10		O	CH <sub>3</sub>	H	3.02
11		O	CH <sub>3</sub>	H	2.42
12		S	CH <sub>3</sub>	H	3.99
13		S	CH <sub>3</sub>	H	4.14
14		S	CH <sub>3</sub>	H	3.71
15		S	CH <sub>3</sub>	H	3.28
16		S	CH <sub>3</sub>	H	3.85

(continued on next page)

Table 1 (continued)

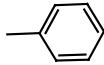
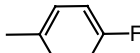
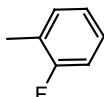
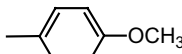
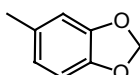
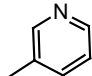
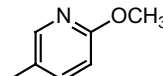
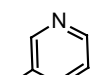
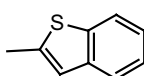
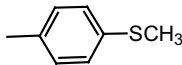
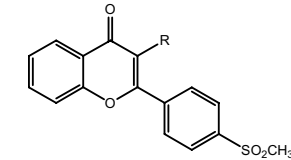
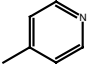
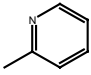
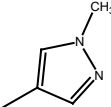
No.	Substitution				$pIC_{50}$
	$R_1$	$R_2$	$R_3$	$R_4$	
17		O	NH <sub>2</sub>	H	3.97
18		O	NH <sub>2</sub>	H	3.90
19		O	NH <sub>2</sub>	H	3.75
20		O	NH <sub>2</sub>	H	3.41
21		O	NH <sub>2</sub>	H	3.03
22		O	CH <sub>3</sub>	H	2.88
23		O	CH <sub>3</sub>	H	2.64
24		O	CH <sub>3</sub>	F	2.90
25		O	CH <sub>3</sub>	H	3.48
26		O	NH <sub>2</sub>	H	3.55

Table 2. Structures of 2,3-diaryl benzopyrans and their COX-2 inhibitory activity (test set)

No.	Substitution	$\log P/(100 - P)$
	R	
1		-3.7046
2		-2.9966
3		-2.6008
4		-3.3257

coefficients is less making a higher  $t$  value hence rendering the terms statistically significant. The observed  $t$  value of the descriptors (4.69)  $vdw\_vol$ , (4.67)  $S\log P\_VSA1$ , (2.45)  $a\_nS$  are greater than the tabulated  $t$  (2.07) at 95% confidence interval.  $S\log P\_VSA1$  is a subdivided surface area descriptor based on approximate accessible van der Waals surface area calculated for each atom. The calculation is based on sum of van der Waals surface area over all atoms with  $\log P(o/w)$  contribution in the range of -0.40, -0.20. Its negative contribution in model-1 indicates that oxygen atom substitution at  $R_2$  position and the pyridinyl ring substitution at  $R_1$  position are not conducive to the activity. Y. H. Joo et al. reported that a nitrogen containing aromatic ring such as pyridine would be a suitable choice for reducing the overt lipophilicity of the compounds but our findings suggests that the substitution by such pyridinyl moiety at  $R_1$  position is detrimental for COX-2 inhibitory activity although it improves the pharmacokinetic profile of the molecule as suggested by the research group.  $a\_nS$  is a function of count of sulfur atoms. Its positive slope suggests the sulfur atom substitution at  $R_2$  position for improved activity. This confirms the significance of s atom at  $R_2$  as suggested by the  $S\log P\_VSA1$  descriptor. The reasonable intercorrelation between these two descriptors also proves that

**Table 3.** Descriptors and the predicted activities of training set molecules through derived QSAR models

No.	Descriptors					Predicted activity (LOO)	
	<i>a_nS</i>	chi0_C	<i>E_oop</i>	<i>S log P_VSA1</i>	<i>vdw_vol</i>	Model-1	Model-2
1	1	14.8119	0.0252	53.8592	487.6671	3.62758	3.48602
2	1	14.6813	0.0251	53.8592	490.8094	3.51652	3.48693
3	1	14.6813	0.0238	53.8592	490.8094	3.47938	3.47541
4	1	14.6813	0.0293	53.8592	490.8094	3.55306	3.46924
5	1	14.6813	0.0262	53.8592	503.6231	3.35055	3.48815
6	1	14.6813	0.0532	53.8592	503.6231	3.35253	3.24634
7	1	14.5518	0.0402	53.8592	519.5790	3.11628	3.40028
8	1	14.5518	0.0593	53.8592	519.5790	3.10378	3.19363
9	1	15.6813	0.0404	53.8592	522.7577	3.08427	3.10393
10	1	15.6813	0.0209	53.8592	512.0963	3.26229	3.34002
11	1	17.3801	0.0818	53.8592	559.6844	2.78469	2.33283
12	2	14.8119	0.0070	49.3138	501.0418	3.94045	3.81922
13	2	14.6813	0.0069	49.3138	504.1841	3.85865	3.83241
14	2	14.6813	0.0055	49.3138	504.1841	3.94702	3.92678
15	2	14.5518	0.0461	49.3138	532.9537	3.56657	3.61816
16	2	15.6813	0.0201	49.3138	536.1324	3.40074	3.45116
17	1	13.8119	0.0259	53.8592	477.4708	3.67233	3.68121
18	1	13.6813	0.0252	53.8592	480.6131	3.63886	3.73107
19	1	13.6813	0.0258	53.8592	480.6131	3.65895	3.74653
20	1	14.6813	0.0449	53.8592	512.5614	3.22638	3.32710
21	1	14.2588	0.0643	53.8592	509.3267	3.29933	3.36186
22	1	14.1048	0.0250	70.6448	478.5916	2.96279	2.82645
23	1	14.9743	0.0323	70.6448	513.6821	2.36261	2.52574
24	1	13.9743	0.0262	70.6448	481.7338	2.88493	2.84835
25	2	14.9659	0.0280	53.8592	528.9142	3.33687	3.39643
26	2	14.6813	0.0593	53.8592	524.2829	3.40907	3.17080

they tend to explain the same phenomenon. The finding suggests a possible weak hydrogen bonding interactions of the sulfur atom at R<sub>2</sub> position with the amino acid residues of COX-2 active site. *vdw\_vol* is the van der Waals volume calculated using a connection table approximation of each molecule. Its negative contribution indicates the steric hindrance due to the increasing size of the molecules. The cross correlation matrix (Table 5) enunciates the orthogonal nature of the descriptors used in model-1. The VIF data from Table 6 depicts the absence of any serious multicollinearity problem among the descriptors.

#### Model-2

$$pIC_{50} = -8.372(\pm 2.850)E_{oop} - 0.250(\pm 0.071)chi0\_C - 0.049(\pm 0.008)S \log P_{VSA1} + 10.010(\pm 1.210)$$

$$n = 26, r = 0.857, r^2 = 0.735, s = 0.246,$$

$$F_{3,22} = 20.30, q^2 = 0.6649, \text{ Spreess} = 0.277,$$

$$SDEP = 0.255, p = 0.000$$

Model-2 is a tri parametric model with overall improved statistical significance. Model-2 explains 73.5% variance

**Table 4.** Descriptors and the predicted activities of test set molecules through derived QSAR models

No.	Descriptors					Predicted activity	
	<i>a_nS</i>	chi0_C	<i>E_oop</i>	<i>S log P_VSA1</i>	<i>vdw_vol</i>	Model-1	Model-2
1	1	14.5517	0.0405	53.8593	519.5790	3.3081	3.3939
2	1	14.1041	0.0598	70.6448	478.5916	3.0520	2.5219
3	1	14.1041	0.0233	70.6448	478.5916	3.0520	2.8273
4	1	13.6899	0.1102	72.2989	477.1550	2.9929	2.1223

**Table 5.** Correlation matrix for the descriptors used in derived QSAR models

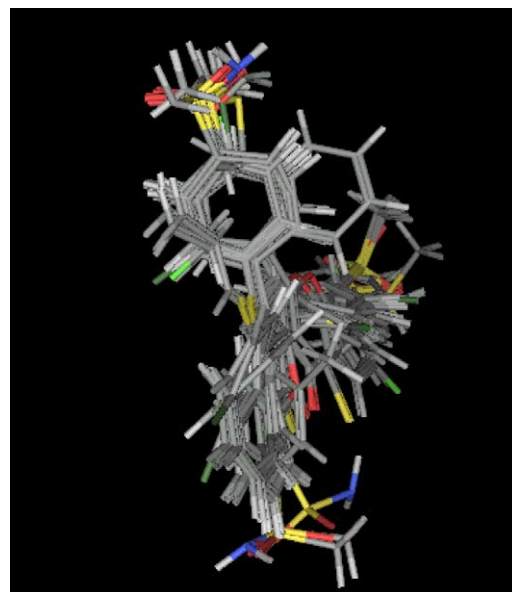
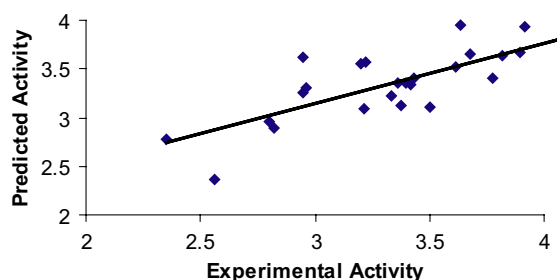
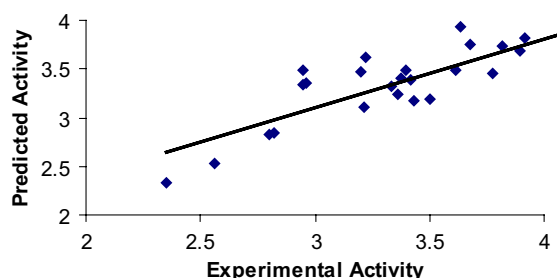
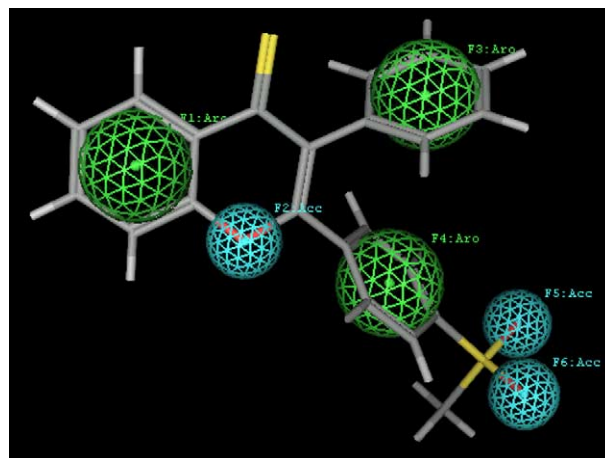
	<i>S log P_VSA1</i>	<i>E_oop</i>	chi0_C	<i>a_nS</i>	<i>vdw_vol</i>
<i>S log P_VSA1</i>	1.000				
<i>E_oop</i>	0.032	1.000			
chi0_C	-0.200	0.341	1.000		
<i>a_nS</i>	-0.440	-0.290	0.101	1.000	
<i>vdw_vol</i>	-0.310	0.549	0.778	0.371	1.000

**Table 6.** VIF test for multi-collinearity among the descriptors for models 1 and 2

	$r^2$	VIF
<i>For model-1</i>		
$S \log P_{VSA1} = -0.050(\pm 0.058)vdw\_vol - 5.052(\pm 2.660)a\_nS + 86.60(\pm 28.42)$	0.218	1.279
$vdw\_vol = 13.27(\pm 9.702)a\_nS - 0.620(\pm 0.724)S \log P_{VSA1} + 523.658(\pm 46.662)$	0.164	1.196
$a\_nS = -0.027(\pm 0.014)S \log P_{VSA1} + 0.006(\pm 0.004)vdw\_vol - 0.130(\pm 2.454)$	0.254	1.340
<i>For model-2</i>		
$S \log P_{VSA1} = -1.919(\pm 1.738)chi0\_C + 37.165(\pm 70.778)E\_oop + 81.973(\pm 24.938)$	0.051	1.054
$chi0\_C = 14.152(\pm 7.786)E\_oop - 0.026(\pm 0.024)S \log P_{VSA1} + 15.715(\pm 1.330)$	0.161	1.192
$E\_oop = 0.000(\pm 0.001)S \log P_{VSA1} + 0.009(\pm 0.005)chi0\_C - 0.115(\pm 0.085)$	0.126	1.144

in activity.  $E\_oop$  is the out of plane potential energy, an internal 3D descriptor.  $chi0\_C$  (topological descriptor) is the carbon connectivity index of order 0. Its negative contribution shows the unfavorable effect caused by the increasing ring size at  $R_1$  position in terms of carbon length. The predictivity of model-2 is also fairly good as reflected from its higher  $q^2$  and low Spres and SDEP values. Figures 2 and 3 depict the self-consistency of both the derived models 1 and 2. In an attempt to corroborate the stability and predictive ability of our derived models, regression equations 1 and 2 are used to predict the  $pIC_{50}$  of four compounds in the test set selected from the original data set with fairly different biological activity data. The predicted  $pIC_{50}$  activities are then compared with the observed ones and are listed in Table 4. The top scoring alignment pattern is indicated in Figure 4.

A pharmacophore query was created in order to identify the pharmacophoric structural features of the active ligands using the pharmacophore Query Editor of MOE. The default scheme used is PCH (polarity-charge-hydrophobicity). Under the PCH scheme, the active

**Figure 4.** Alignment pattern of all 26 compounds as training set used for QSAR study.**Figure 2.** Predicted versus experimental ( $pIC_{50}$ ) values of compounds for model-1.**Figure 3.** Predicted versus experimental ( $pIC_{50}$ ) values of compounds for model-2.**Figure 5.** Probable pharmacophore features of active molecule-12.

molecule 12, shown in Figure 5, has six annotation points, [F1–F6]. The annotation contains label *Aro* attached to point F1, F3, and F4; label *Acc* attached to points F2, F5, and F6. Under this scheme, *Aro* denotes an aromatic ring probe, *Don* denotes an H-bond donor, and *Acc* denotes an H-bond acceptor, *Cat* denotes the cations, *Ani* denotes the anions, and *Hyd* denotes hydro-

phobic areas. Different pharmacophores developed are in good agreement with previously published pharmacophores under the individual diaryl heterocyclic compounds developed as novel selective COX-2 inhibitors.<sup>16</sup>

In our QSAR investigations, the two models developed for 26 compounds and validated against four test set compounds discerned some important structural insights to aid the design of new potent selective COX-2 inhibitors. Model-1 suggests a sulfur atom substitution at position R<sub>2</sub> for improved activity and the negative contribution of the volume descriptor suggests that the COX-2 receptor site has a limited tolerance to bulk of the R<sub>1</sub>, R<sub>2</sub>, R<sub>3</sub>, and R<sub>4</sub> interacting groups. The topological parameter of model-2 confirms the significance of the steric hindrance caused by the increasing ring size at R<sub>1</sub> position in terms of carbon length. Pharmacophore query demonstrated two aromatic probes; an acceptor probe and a sulfonyl probe as the key pharmacophore features for selective COX-2 inhibition for these classes of ligands.

### Acknowledgements

Authors S.P. and E.M. thank the University Grants Commission (UGC), New Delhi for the financial support for this research and the Tata elxsi, India for providing the MOE software. We wish to thank Dr. E. Sobhia and Mr. V. Raja Solomon for their helpful guidance.

### References and notes

1. Allison, M. C.; Howatson, A. G.; Torrance, C. J.; Lee, F. D.; Russell, R. I. *N. Engl. J. Med.* **1992**, 327, 749.
2. Kujubu, D. A.; Fletcher, B.; Varum, B. C.; Lim, R. W.; Herschman, H. R. *J. Biol. Chem.* **1991**, 266, 12866.
3. Vane, J. R.; Mitchell, J. A.; Appleton, I.; Tomlinson, A.; Bishop-Bailey, D.; Croxtall, J.; Willoughby, D. A. *Proc. Natl. Acad. Sci.* **1994**, 91, 2046.
4. Kurumbail, R. G.; Stevens, A. M.; Gierse, J. K.; McDonald, J. J.; Stegeman, R. A.; Pak, J. Y.; Gildehaus, D.; Miyashiro, J. M.; Penning, T. D.; Seibert, K.; Isakson, P. C.; Stallings, W. C. *Nature* **1996**, 384, 644.
5. Vane, J. R. *Nature* **1994**, 367, 215.
6. Prescott, S. M.; Fitzpatrick, F. A. *Biochim. Biophys. Acta* **2000**, 1470, M69.
7. Reddy, B. S.; Hirose, Y.; Lubet, R.; Steele, V.; Kelloff, G.; Paulson, S.; Seibert, K.; Rao, C. V. *Cancer Res.* **2000**, 60, 293.
8. Kumar, R.; Singh, P. *Indian J. Chem.* **1997**, 36B, 1164.
9. Singh, P.; Kumar, R. *J. Enzyme Inhib.* **1999**, 14, 277.
10. Desiraju, G. R.; Gopalakrishnan, B.; Jetti, R. K. R.; Ravendra, D.; Sarma, J. A. R. P.; Subramanya, H. S. *Molecules* **2000**, 5, 945.
11. Chavatte, P.; Yous, S.; Marot, C.; Baurin, N.; Lesieur, D. *J. Med. Chem.* **2001**, 44, 3223.
12. Roy, K.; Chakraborty, S.; Saha, A. *Bioorg. Med. Chem.* **2003**, 21, 3753.
13. Garg, R.; Kurup, A.; Meakapati, S. M.; Hansch, C. *Chem. Rev.* **2003**, 103, 703.
14. Joo, Y. H.; Kim, J. K.; Kang, S.-H.; Noh, M.-S.; Ha, J.-Y.; Choi, J. K.; Lim, K. M.; Lee, C. H.; Chung, S. *Bioorg. Med. Chem. Lett.* **2003**, 13, 413.
15. Saxena, A. K.; Ram, S.; Saxena, M.; Singh, N.; Prathipati, P.; Jain, P. C.; Singh, H. K.; Anand, N. *Bioorg. Med. Chem.* **2003**, 11, 2085.
16. Palomer, A.; Cabre, F.; Pascual, J.; Trujillo, M. A.; Entrena, A.; Gallo, M. A.; Garcia, L.; Mauleon, D.; Espinosa, A. *J. Med. Chem.* **2002**, 45, 1402.